(4) Taniguchi, M.; Yamagishi, A. *Inorg. Chem.* **1991**, *30*, 2462.
(5) Mezey, P. G. *ACS Symp. Ser.* **1984**, *248*, 145.
(6) (a) Ramadas, S.; Thomas, J. M.; Betteridge, P. W.; Cheetham, A. K.; Davies, E. K. *Angew. Chem., Int. Ed. Engl.* **1984**, *23*, 671. (b) Vega, L.; Breton, J.; Girardet, C.; Galatry, L. *J. Chem. Phys.* **1986**, *84*, 5171. (c) Skipper, N. T.; Refson, K.; Mcconnell, J. D. C. *Clay Minerals* **1989**, *24*, 411. (d) Gale, J. D.; Cheetham, A. K.; Jackson, R. A.; Catlow, C. R.; Thomas, J. M. *Adv. Mater.* **1990**, *2*, 487.
(7) Sato, H.; Yamagishi, A.; Kato, S. *Clay Sci.* **1991**, *8*, 147.
(8) Kato, S.; Amadatsu, Y. *J. Chem. Phys.* **1990**, *92*, 7241.
(9) Zalkin, A.; Templeton, D. H.; Ueki, T. *Inorg. Chem.* **1973**, *12*, 1641.
(10) Gibbs, G. V. *Am. Mineral.* **1982**, *67*, 421.
(11) Allen, M. P.; Tildesley, D. J. *Computer Simulation of Liquids*; Oxford University Press: Oxford, 1987.
(12) Ando, K.; Kato, S. *J. Chem. Phys.* **1991**, *98*, 5966.
(13) Joshi, V.; Ghosh, P. K. *J. Am. Chem. Soc.* **1989**, *111*, 5604.

Molecular Recognition on Acoustic Wave Devices: Sorption in Chemically Anchored Zeolite Monolayers

Yongan Yan and Thomas Bein*

Department of Chemistry, Purdue University, West Lafayette, Indiana 47907 *(Received: February 10, 1992; In Final Form: August 3, 1992)*

Zeolite crystals were attached to the gold electrodes of quartz crystal microbalances (QCM). Monolayers of thiol–alkoxysilanes on the gold surface served as interfacial layers for the subsequent adhesion of the zeolite crystals to the QCM. The process of anchoring the zeolite crystals via the thiol–silane monolayers was studied by reflection adsorption infrared (IR) spectroscopy, contact angle, and scanning electron microscopy (SEM). The siloxane linkages between the microporous zeolite crystals and the terminal cross-linked polysiloxane groups of the interfacial monolayer play an important role in enhancing the packing density of microporous crystals and the thermal stability (up to at least 350 °C) of the film on the gold surface. Dynamic sorption isotherms of organic vapors and nitrogen as well as the transient sorption behavior of organic vapor pulses were studied to characterize the zeolite-coated QCMs. The resonance frequency response of zeolite-coated QCMs to vapor pulses could be increased up to 500-fold compared to the bare sensor. The regular micropores (0.3–0.75 nm) of the QCM-attached zeolite crystals were found to efficiently control molecular access into the coating. Selectivity of the frequency response in excess of 100:1 toward molecules of different size and/or shape could be demonstrated. The kinetics of vapor desorption from the zeolite layers are strongly dependent on the adsorbate/zeolite combination, thus providing an additional capability for molecular recognition.

Introduction

The design of selective coatings for microsensors such as optical waveguides, chemically sensitive field effect transistors, chemiresistors, and acoustic wave devices has attracted growing attention.[1-3] The goal of these studies is to increase the sensitivity and chemical selectivity of the sensor by controlling the surface interactions and solubilities of analyte vapors to be detected.

Our recent development of molecular sieve-based composite films has introduced a novel means for tailoring vapor/surface interactions.[1,4-6] A sensor coated with molecular sieve crystals not only detects vapors by the adsorption of target molecules but also discriminates different molecules according to their sizes and shapes. Our previous work was focused on zeolite/glass microcomposites derived from sol/gel suspensions that were coated on surface acoustic wave devices. The zeolite-coated microsensors provide a molecular sieving function, with the ability to fine-tune pore opening sizes in the range 0.3–1.2 nm to detect compounds with different molecular kinetic diameters. Furthermore, these coatings also offer the ability to control vapor/surface interactions through acid/base and polar properties of the molecular species of interest. However, even though zeolite/glass composites have favorable stability, the glass matrix can introduce additional nonselective porosity and/or obstruct part of the zeolitic porosity.

As part of our efforts to extend the control of vapor/surface interactions and to optimize the preparation of selective coatings, this article reports the anchoring of microporous crystals through a molecular interface. The coupling agent (3-mercaptopropyl)-trimethoxysilane, $HS(CH_2)_3Si(OCH_3)_3$, was used as a bifunctional molecular precursor for anchoring zeolite crystals to the gold electrode. Gold shows strong specific interactions with thiol groups that permit formation of self-assembled monolayers in the presence of many other functional groups.[7-10] Figure 1 summarizes the idealized process of the formation of a zeolite-coated QCM. A related system consisting of SnO_2/cationic disilane/zeolite arrangements has been reported for the self-assembly of redox chains on electrodes.[11] Grazing angle reflection absorption-FTIR, contact angle measurements, and electron microscopy were used to study the process of coupling zeolite crystals to the gold surface with molecular-level control over the interfacial chemistry. We further demonstrate the unique sorption features of the zeolite-coated QCMs which are derived from the transient sorption of vapor pulses and dynamic sorption isotherms.

The QCM is based on a piezoelectric quartz substrate coated with keyhole pattern electrodes on opposite surfaces of the crystal. Mass changes Δm (in grams) per face of the QCM cause proportional shifts Δf of the fundamental resonance frequency F, according to

$$\Delta f = -2.3 \times 10^{-6} F^2 \Delta m / A$$

where A is the electrode surface area (in cm^2). It follows that the 9- or 5-MHz QCM is capable of detection of mass changes at the nanogram level.[12-15] Two types of surface area can be distinguished on the zeolite-coated QCM electrodes: the external surface area which consists of the zeolitic external surface and the electrode surface exposed to the gas phase and the internal zeolite surface area that is only accessible to molecules smaller than the micropore opening size. If 90% of the electrode is covered by 5-μm crystals of CaA zeolite, the ratio of N_2 sorption at liquid nitrogen temperature on the internal and external surface would be expected to exceed 1000.[16] This ratio is an estimate for the possible discrimination/selectivity of organic vapors to be expected on the coated QCM.

Experimental Section

Materials. Potassium A zeolite was obtained by 3-fold exchange of 4A zeolite (5.0 g, Alfa) with 1 N aqueous solution of KCl (80 mL, 20 °C, 8 h) and subsequent filtering and washing with water (5-fold). Sodium zeolite Y with SiO_2/Al_2O_3 molar ratio of 4.74

* To whom correspondence should be addressed.

0022-3654/92/2096-9387$03.00/0

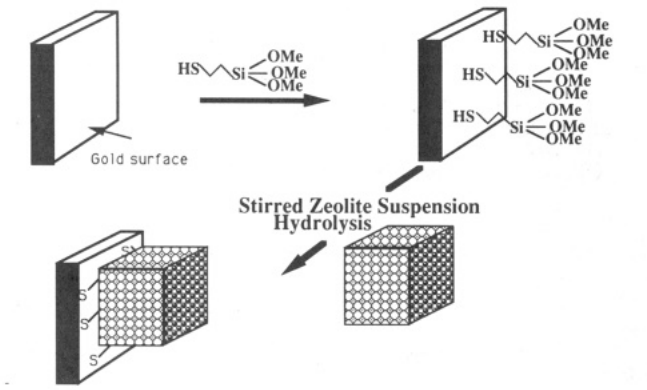

Figure 1. Anchoring of zeolite crystals on a gold surface via the thiol–alkoxysilane interfacial layer.

and silicalite with SiO_2 content >99% were obtained from Union Carbide and used as received. $HS(CH_2)_3Si(OCH_3)_3$ (MPS) (Aldrich) was used without further purification. Toluene and hexadecane (Fisher) were stored over dehydrated 3A zeolite and deoxygenated by bubbling N_2 for 30 min when employed as solvents for the formation of organosilane–thiol monolayers.

Attachment of Zeolite Crystals to Gold Surfaces. Gold substrates were prepared by thermal evaporation of high-purity gold (99.999%, Aldrich) onto 7.5 × 2.5 cm^2 microscope glass slides (Fisher), which had been precleaned with 7:3 concentrated H_2SO_4/H_2O_2 mixture and precoated with chromium to improve adhesion. These gold substrates were used for reflection absorption IR, contact angle, and SEM characterization. The vacuum-deposited gold electrodes on the AT-cut 5 MHz QCMs acquired from ICM-Crystal Division (Oklahoma) were used for zeolite coating, porosity characterization, and selectivity studies with different organic vapors. The gold substrates were plasma-cleaned (5 min O_2, 6–8 Torr and 3 min N_2, 6–8 Torr) before use. The anchoring of zeolite crystals to the gold surface involved two steps: formation of the thiol monolayers and exposure to a zeolite suspension in toluene or acetonitrile. The thiol monolayers were spontaneously formed by immersing the gold substrate into 1.0–5.0 mM (3-mercaptopropyl)trimethoxysilane (MPS) solution in dry hexadecane or toluene.[9,10,17] It was found that 40–60-min reaction time was sufficient to form the thiol monolayer as indicated by the contact angle reaching a constant value.

The monolayer-covered slides were rinsed with toluene or acetonitrile to remove excess adsorbate from the gold substrate, transferred to a presonicated suspension of 0.1 g of zeolite in 30 mL of toluene or acetonitrile, and stirred overnight. After attachment of the zeolite crystals, the alkoxy groups of the silane were hydrolyzed and further reacted with the zeolite by heating in air at 100 °C for 1 h. The coverage of the QCMS with zeolite crystals (typically 20–30 $\mu g/cm^2$; given in the figure captions) was determined by measuring the frequency of dry QCM crystals before and after zeolite attachment.

Reflection Absorption Infrared Spectroscopy. Reflection absorption infrared spectra (RAIR) were obtained by reflection of a p-polarized beam from the gold surface at the near-glancing angle of incidence of 87°.[18,19] A Mattson Polaris FTIR spectrometer was equipped with a RAIR attachment (Harrick) and a liquid nitrogen cooled narrow band MCT detector and operated at a resolution of 4 cm^{-1}. Uncoated gold substrates that had been cleaned as above immediately before the measurement were used for the acquisition of background spectra. The samples were transferred and mounted in the spectrometer under purified nitrogen to minimize adsorption of water and other contaminations.

Contact Angle Measurement. Contact angles were determined with sessile drops on the respective substrates in a microscope equipped with an environment-controlled transparent chamber. The advancing water contact angle $\phi_a(H_2O)$ was obtained by measuring the tangent to a 2-μL drop at its intersection with the surface.[9] The relative humidity was maintained at 100% by filling wells in the sample chamber with distilled water. The average value of six measurements taken at different locations on the film surface showed a maximum standard deviation of ±3°.

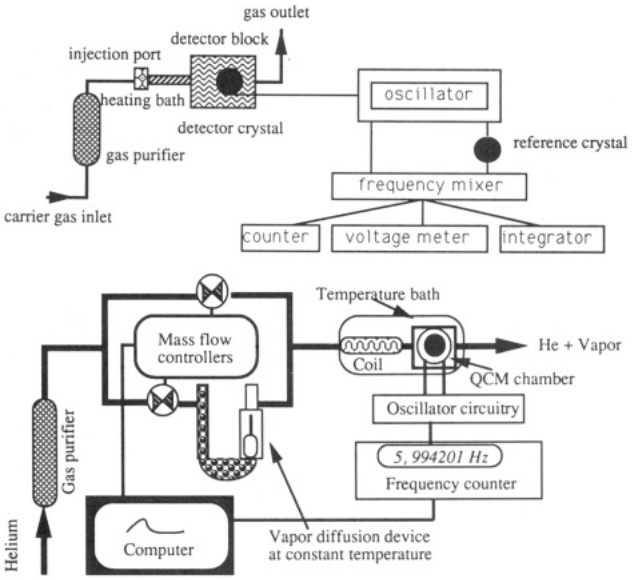

Figure 2. (A, top) Schematic diagram of the apparatus for transient sorption of vapor pulses by zeolite-coated QCM. (B, bottom) Schematic diagram of the apparatus for vapor sorption isotherms by zeolite-coated QCM.

Scanning Electron Microscopy. SEM micrographs were obtained on a Hitachi S800 scanning electron microscope using a 15-kV potential. Prior to microscopic examination, the samples were sputter-coated with carbon to provide a conductive surface.

Characterization of Coating Porosity. *Sorption of Vapor Pulses.* The response of the zeolite-coated QCMs to different vapor pulses was examined with a modified Perkin-Elmer Sigma 2 gas chromatograph, schematically shown in Figure 2A. A carrier gas (He or N_2), purified by passing through a molecular sieve trap, continuously purges the injection port and detector cells. All zeolite-coated QCMs were heated to 150 °C to remove water prior to use. IR spectroscopic and sorption measurements established that this treatment reduces the water content in the thin zeolite films below detection level. The liquid samples (0.5 μL) were injected through a temperature-controlled injection port, whose temperature was 30–50 deg higher than the detectors to ensure fast evaporation and avoid condensation. The vapor leaving from the injection port was then passed through a 1-mL Teflon-sealed brass cell housing the QCM. The frequency variation was monitored by heterodyning the QCM frequency changes against a reference oscillating circuit in a frequency mixer and converter to an analog voltage. The frequency output was simultaneously monitored by a frequency counter (HP 5384A) and recorded by an integrator (HP 3380A). The QCM response to vapor pulses was compared with that of a thermal conductivity detector (TCD) in series with the QCM.

Dynamic Sorption Isotherms. Vapor sorption isotherms at 85 °C were measured in a computer-controlled gas flow system with mass flow controllers (UNIT) (Figure 2B). The QCMs were degassed at 150 °C for vapor sorption and 200 °C for nitrogen sorption. Purified UHP helium was passed through a saturation device containing gravimetrically calibrated vapor diffusion tubes. The vapor partial pressure was adjusted by variation of the flow rate and further dilution with a second helium stream. The vapor was then passed through a temperature equilibration coil and into a 1-mL Teflon-sealed cell, containing the coated QCM. The frequency variations of the oscillator circuitry were continuously read by the computer until below a predetermined threshold when the system was considered sufficiently close to equilibrium. Vapor sorption isotherms performed on the different QCMs with zeolites were reproducible within better than 10%. Nitrogen adsorption isotherms were obtained at −196 °C in a second similar gas dosing system with computer-adjusted mass flow controllers. The nitrogen partial pressure in helium was adjusted over the range 0–0.95. The stability of the QCM resonance frequency was better

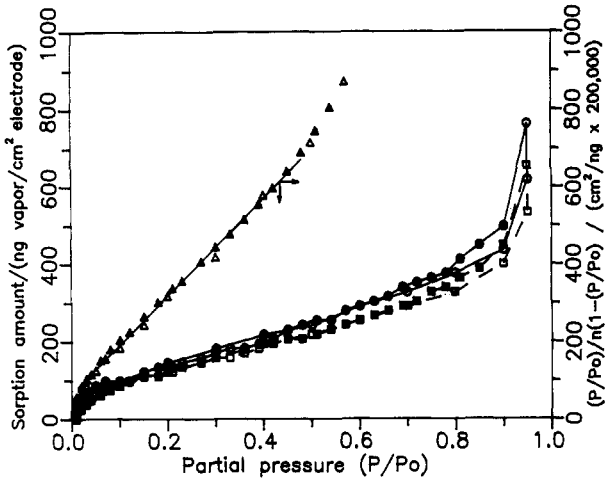

Figure 3. Nitrogen sorption on QCM gold electrode (at −196 °C). (A) BET plot, △; (B) adsorption isotherm on bare QCM, ○; (C) adsorption isotherm on MPS-coated QCM, □.

than 1 Hz over 20 min at both the high and low temperatures used.

Results and Discussion

Formation of the Zeolite Crystal-Coated QCM. The external surface area due to the roughness of the gold electrode of the bare QCM after plasma cleaning was determined from the nitrogen sorption isotherm at liquid nitrogen temperature. By varying the partial pressure of nitrogen in the helium/nitrogen flow, a nitrogen sorption isotherm can be obtained in the form of a QCM frequency shift vs partial pressure, which is converted to the mass adsorbed on the electrode as a function of the partial pressure (Figure 3B). The sorption shows the characteristics of the type II isotherm, and the associated nitrogen monolayer sorption capacity was derived from the BET equation[20-22]

$$n/n_m = c(P/P_0)/\{(1 - P/P_0)[1 + (c - 1)P/P_0]\}$$

where n is the amount adsorbed at partial pressure P/P_0, n_m the monolayer capacity, and c a constant at the given temperature. Figure 3A shows the plot of $(P/P_0)/n(1 - P/P_0)$ against P/P_0. A linear relation holds in the partial pressure range 0.01–0.45. The nitrogen monolayer capacity is consequently calculated from the plot according to

$$n_m = 1/(s + i) \quad \text{and} \quad c = 1 + s/i$$

where s is the slope and i the intercept by extrapolation to zero. A nitrogen monolayer capacity of 75 ng/cm² was obtained, which corresponds to 2.6 cm²/cm² external surface area on the QCM gold electrode.

For the QCM coated with coupling agent MPS, a mass increase of 0.29 μg/cm² could be observed when the MPS adsorption was carried out under nitrogen. Taking into account the electrode surface area of 2.6 cm²/cm², this coverage relates to an effective cross section of 30 Å² for the MPS molecules for a single layer adsorption. (A densely packed methylene chain has a cross section of about 20 Å².[10]) When the coating process was performed in ambient air, and the MPS-coated QCMs were not immediately rinsed in toluene and purged in a nitrogen flow, mass increases of about 0.40–0.60 μg/cm² were obtained. The increased adsorption in the latter case probably results from the partial oligomerization of the MPS during attachment to the electrodes. The nitrogen sorption isotherm (Figure 3C) on the QCM coated with the MPS coupling layer indicates a 14% decrease in the surface area compared to the case of the bare QCM. This shows that no new porosity was created after the formation of the MPS coupling layer and indicates filling of some fraction of the gold pores with MPS.

IR spectra of the thiol monolayer formed on gold show several characteristic vibrational bands of MPS. A band at 2961 cm⁻¹ is assigned to the asymmetric in-plane CH stretching mode of the OCH_3 groups, $\nu_a(CH_3\text{-ip})$, and the band at 1195 cm⁻¹ to the rocking mode of the same group. Bands at 2930 and 2847 cm⁻¹ correspond to the methylene ν_a and ν_s modes, respectively. A very strong peak at 1115 cm⁻¹ is due to the Si–O–C asymmetric stretching vibration, ν_a(Si–O–C).[10,17,23,24] For comparison, peak positions for the spectra of the bulk phase of $HS(CH_2)_3Si(OCH_3)_3$ are also given in Table I.

TABLE I: IR Spectral Mode Assignments of $HS(CH_2)_3Si(OCH_3)_3$, Neat and Adsorbed on Gold

peak positions (cm⁻¹)			
on gold	neat[a]	assignment	ref
2961 sh		$\nu_a(CH_3\text{-ip})$	10, 17
2930	2937	$\nu_a(CH_2)$	10, 17
2847	2840	$\nu_s(CH_2)$	23, 24
1461	1455	$\delta_a(CH_3;CH_2)$	23, 24
1195	1190	$\rho(CH_3)$	23, 24
1115	1117	ν_a(Si–O–C)	23, 24
	1069	ν_s(C–O)	23, 24

[a] $HS(CH_2)_3Si(OCH_3)_3$ between NaCl windows. Abbreviations: ν, stretching; δ, bending, ρ, rocking.

After hydrolysis of the surface-assembled thiol monolayer at 70 °C, the peak intensities of the methoxy vibrations decreased. It was observed that the methylene peak intensities also dropped during the heat treatment. These changes may be due to evaporation of some physisorbed coupling agent or due to different methylene group orientations after siloxane cross-linking. If the methylene chains orient more perpendicular to the gold surface, the HCH planes will be more parallel to the surface which would reduce the peak intensity due to the surface IR selection rules.

Figure 4 presents SEM micrographs of the zeolite-coated gold surfaces. It is clear that this coating process provides a method to obtain uniform crystal distributions on the entire slide surface. The attached particles also display the crystalline habit of the bulk materials. For the crystals with noncubic shape, for example, silicalite (Figure 4B), one of the larger crystal faces is preferentially attached to the silane–thiol layer. We note that the coating process is independent of the slide orientation in the suspension, i.e., whether the slide is oriented vertically or at an acute angle. It was also discovered that *no zeolite crystals attached on the fresh gold surface without the silane–thiol layer.* The zeolite coating on thermally treated slides can partially survive low power ultrasonication. When the zeolite-coated QCM was heated to 350 °C, no significant mass change was observed after reequilibration in air.

For the fresh plasma-cleaned gold slide, water contact angles $\phi_a(H_2O)$ of 12–14° were observed. This is comparable to 0–8° reported for clean gold.[25] For the $HS(CH_2)_3Si(OCH_3)_3$ monolayer on gold, $\phi_a(H_2O)$ reached a constant value of 53° after immersing the slide in the thiol solution for more than 40 min. This value is significantly lower than that for the methyl-terminated monolayer of long CH_2 chains (114°)[8] and reflects the presence of the terminal $Si(OCH_3)_3$ groups on the surface. After an hydrolysis treatment in air at 100 °C, $\phi_a(H_2O)$ increased to 81°. This increase is related to the formation of the polysiloxane/silanol surface. After anchoring the zeolite crystals on the slides, $\phi_a(H_2O)$ of 67° and 78° were obtained respectively for NaY and silicalite-coated slides. (Values between 44° and 84° have been reported on porous silica glass.[26])

Sorption on Zeolite-Coated Quartz Microbalances. *Nitrogen Sorption Isotherms.* The pore opening sizes of the microporous coatings vary from the partially potassium blocked, 8-oxygen-membered ring of 3A zeolite (0.3 nm) to 10-ring silicalite (0.55 nm) and of sodium Y zeolite with 12-membered rings (0.75 nm). The Si/Al ratios increase from 1.0 for A zeolite, 2.4 for Y zeolite, to ca. 100 for silicalite. The intrazeolite surface changes from hydrophilic to hydrophobic in the same sequence.[27,28]

The nitrogen sorption isotherms at −196 °C of the above films are presented in Figure 5. The sorption is characterized by reversible isotherms for all three zeolites, with some parallel hysteresis on Y and silicalite, indicating a small fraction of mesoporosity. It requires 10–80 min to return from the last data point back to zero nitrogen loading. The significant uptake at

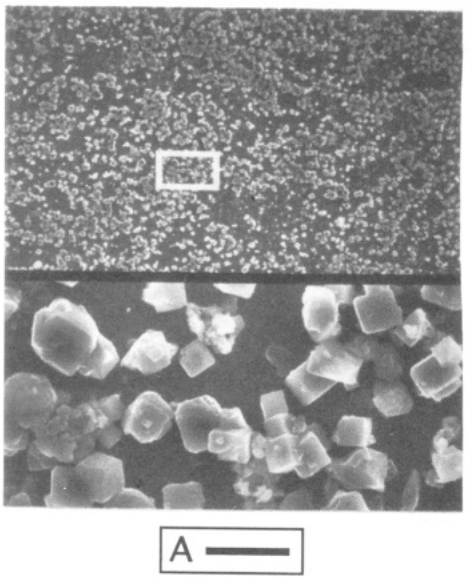

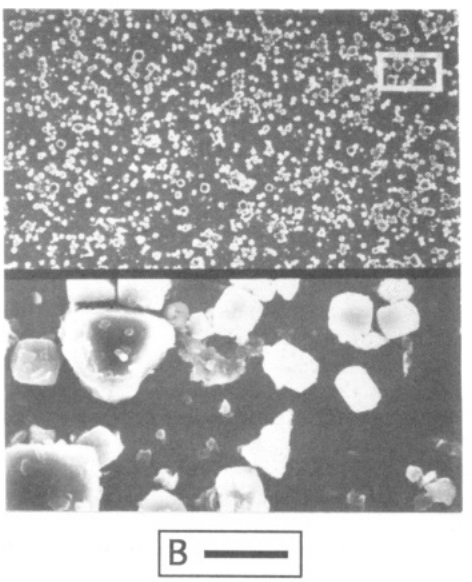

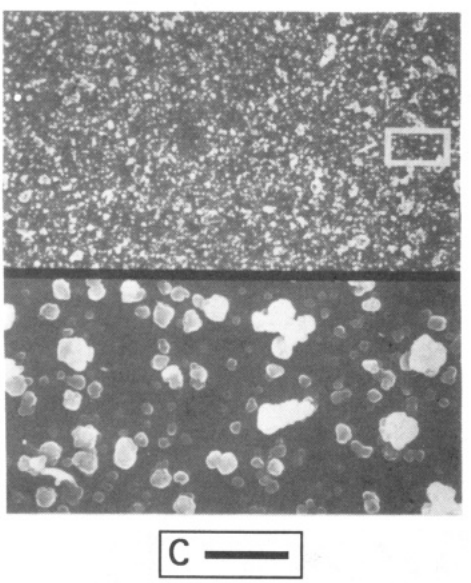

Figure 4. Scanning electron micrographs of zeolite crystals anchored to gold surfaces via the interfacial coupling layer, after ultrasonication: (A) zeolite 3A, (B) silicalite, (C) zeolite NaY. Scale bar: 50 μm (top part); 5 μm (bottom part). The frame indicates the area of higher magnification.

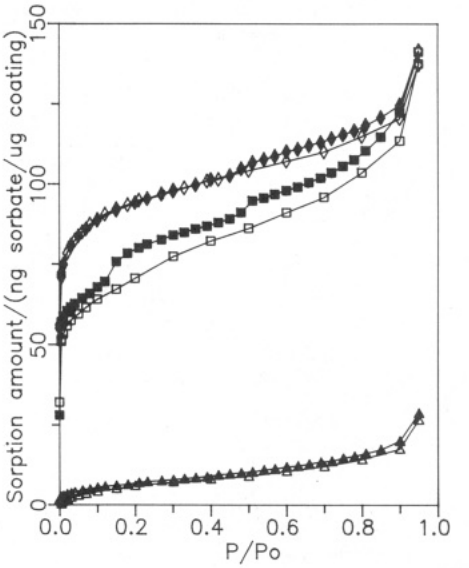

Figure 5. Sorption isotherms of nitrogen at −196 °C on QCMs coated with zeolite 3A (25.6 μg/cm^2) (△), silicalite (32.8 μg/cm^2) (□), and zeolite NaY (16.1 μg/cm^2) (◇). Open and filled symbols designate sorption and desorption points, respectively.

TABLE II: Porosity Analysis of the Zeolite Thin Films by α_s Plots

	N_2 sorption on microporous fraction			N_2 monolayer sorption on external surface of thin film	
	thin film		bulk material		
	in g/g	in cm^3/g[a]	in g/g	in g/g	in m^2/g[b]
zeolite 3A			<0.01 (ref 31)	0.004	13
silicalite	0.059	0.073	0.17 (ref 30)	0.026	91
zeolite NaY	0.078	0.097	0.25 (ref 31)	0.015	52

[a] The density of liquid nitrogen at −196 °C is 0.808 g/cm^3. [b] Nitrogen molecular area is taken as 16.2 Å^2; the slope for the α plots of the desorption branch was evaluated between ca. 0.1 and 0.4P/P_0.

low partial pressures on the Y and silicalite films indicates microporosity which is characteristic for the bulk zeolites. In contrast, the isotherm of 3A is type II, showing the expected absence of microporous adsorption for nitrogen due to size exclusion.

A more detailed porosity analysis of the zeolite thin films can be provided by the α_s plot results listed in Table II. The principle of the t or α_s plot is based on the assumption that characteristic amounts of gas per unit area are adsorbed at a given partial pressure on nonporous materials with similar surface interactions.[29] Departure from such reference isotherms is interpreted in terms of micropore filling. The nonmicroporous surface used for the reference isotherm should have similar chemical properties and a similar BET c constant as the solid under consideration. In the present study the sorption isotherm of silica[21] (sorption of nitrogen at $P/P_0 = 0.4$ is 15.5 μmol m^{-2}) was used as the reference for the α_s plot of the sorption isotherm on silicalite films. Because the zeolite A film is chemically similar to zeolite Y film and shows no microporosity for nitrogen, the isotherm of zeolite A film was used as reference for the α_s plot of sorption on zeolite Y film. The nitrogen micropore sorptions are 0.059 g/g for silicalite and 0.078 g/g for Y. These values are of the same order but lower than for the bulk systems (0.17 for silicalite,[30] 0.25 g/g for NaY[31]).

Beyond the partial pressure range associated with micropore filling, both isotherms are not as horizontal as in the bulk but continue to rise to 0.113 and 0.120 g/g at relative pressure 0.9, respectively. At least for zeolite Y, this adsorption must be on external surface area (or macropores), as the isotherm shows that mesopores do not play a significant role.

The silicalite thin films show the largest external area,[30] which can be attributed to irregular crystal morphology and the presence of amorphous phase. If the nitrogen uptake of a 3A-coated QCM (which should not adsorb nitrogen into the pore system) and that of a bare QCM are compared, we find that the zeolite coating

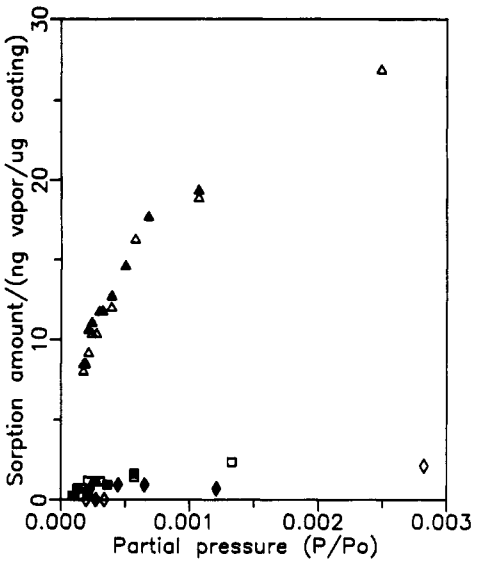

Figure 6. Sorption isotherms of water (△, P_0 = 434 Torr), *n*-hexane (□, P_0 = 1233 Torr), and isooctane (◇, P_0 = 499 Torr) on a QCM coated with zeolite 3A (25.6 $\mu g/cm^2$) at 85 °C. Total pressure is 1 atm.

does not increase the external surface area of the QCM electrode to a great extent. For the QCM coated with 25.6 $\mu g/cm^2$ zeolite 3A, the external surface increases from 2.6 cm^2/cm^2 on the bare QCM to 4.2 cm^2/cm^2.

Several factors can contribute to some loss of microporosity in the thin films. If not all crystals are acoustically coupled to the QCM, the isotherms should be type I like the bulk materials but with reduced microporosity. Because there is further adsorption at higher pressures, small or irregular zeolite crystals and/or nonporous matter on the QCM apparently increase the relative importance of external adsorption compared to bulk powders.

Vapor Sorption in Zeolite Layers. *Zeolite 3A.* Equilibrium sorption data of the probe molecules in the zeolite films were determined in a stream of diluted vapors at 85 °C. The host with the smallest pore size used in this study, zeolite 3A, would be expected to adsorb only water (kinetic diameter 0.265 nm), but not *n*-hexane (0.43 nm) and isooctane (2,2,4-trimethylpentane, 0.62 nm) into the pore system. An additional driving force for the adsorption of water is the highly polar internal surface of zeolite A; thus, the uptake at very small partial pressures should be substantial.

The equilibrium sorption data confirm the expected behavior: The uptake of water, *n*-hexane, and isooctane is 0.019 (at P/P_0 = 0.0011), 0.002 (P/P_0 = 0.0013), and 0.001 g/g (P/P_0 = 0.0012), respectively (Figure 6). Only water can fit into the zeolite 3A pores; adsorption of the other molecules must occur on the much smaller external surface of the zeolite composite film. Therefore, the response to larger molecules is reduced by a factor of at least 10. Accordingly, adsorption in the bulk zeolite 3A powder is only observed for water (ca. 0.28 g/g at saturation), but not for the other molecules. This value cannot be directly related to the QCM data because much lower partial pressures and different temperatures have been used in the QCM experiments.

In contrast to bulk zeolite materials, the adsorption behavior of water in the polar zeolite films containing zeolite 3A (and NaY) shows fast, reversible attainment of equilibrium. Complete desorption of water can be achieved at 100 °C in less than 5 min, and the adsorption equilibrium of the isotherm can be reached in 30 s irrespective of the type of zeolite.

The transient adsorption of different organic vapor pulses on zeolite 3A-coated quartz microbalances was studied. Figure 7 shows the responses of 3A zeolite-coated QCMs upon sequential injection of 0.5 μL of different liquids at 100 °C. For comparison, the corresponding signals of a thermal conductivity detector (TCD; in series with the QCM) and of the bare QCM are also illustrated.

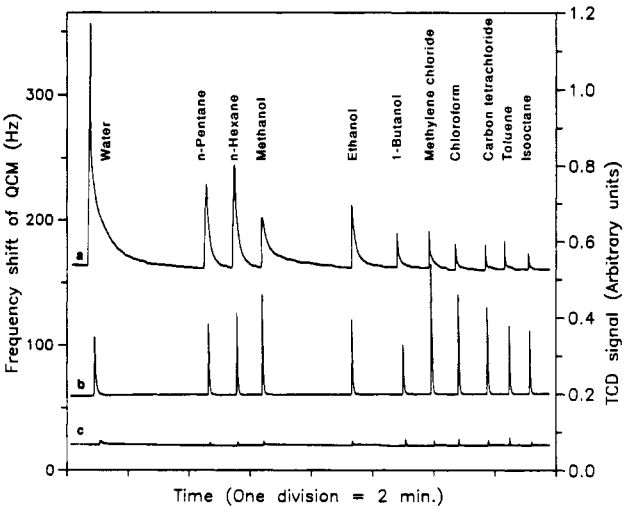

Figure 7. Transient sorption of vapor pulses on a QCM coated with 16.2 $\mu g/cm^2$ zeolite 3A, at 100 °C (frequency shifts correspond to QCM coated on both sides): (a) frequency shift of QCM/zeolite film, (b) TCD signal, (c) frequency shift of uncoated QCM.

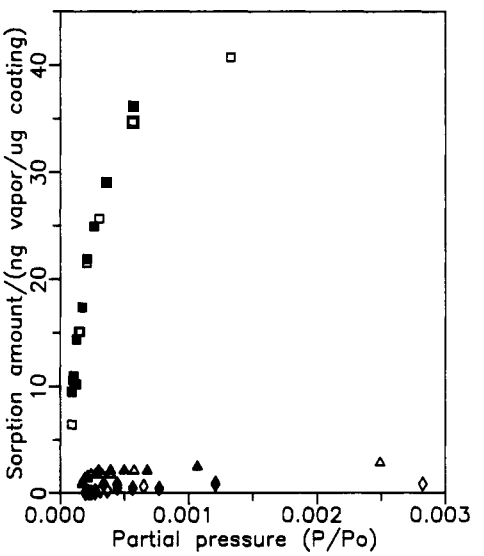

Figure 8. Sorption isotherms of water (△), *n*-hexane (□), and isooctane (◇) on a QCM coated with silicalite (32.8 $\mu g/cm^2$) at 85 °C.

The preferential adsorption of water is clearly seen, but vapors of other small molecules (e.g., MeOH or *n*-hexane) also show some adsorption. This adsorption must be due to coverage of external surfaces or macropores at the high partial pressures of the pulses, as the adsorption isotherms discussed above show a much greater selectivity for water at low partial pressures (compare, e.g., water vs *n*-hexane). The pulse-shaped TCD traces demonstrate that the tails observed in the QCM response to several vapors are not due to the mixing time constant of the QCM cell, but rather related to desorption from the film (see below).

Silicalite. The pore sizes of silicalite are larger than those of zeolite 3A (0.55 nm); based on size, adsorption of water and *n*-hexane but not of isooctane is therefore expected. The adsorption isotherms confirm a significant uptake of *n*-hexane (0.040 g/g at P/P_0 = 0.0013; bulk at saturation 0.13 g/g)[27] (Figure 8). However, water is only adsorbed at about 5% of that value in the film (0.002 g/g; bulk at saturation 0.05 g/g).[27] The low affinity of the hydrophobic silicalite sieve toward water is clearly apparent. If the molecular size is increased beyond the diameter of the pore openings (isooctane), the uptake goes to almost zero (0.001 g/g at P/P_0 = 0.0012).

Figure 9 shows the frequency shifts of the silicalite-coated QCM in response to vapor pulses. If the responses of the silicalite layer (29.6 $\mu g/cm^2$) to water (0.265 nm) and isooctane (0.62 nm) are compared, the discrimination ratio of the molecules admitted and

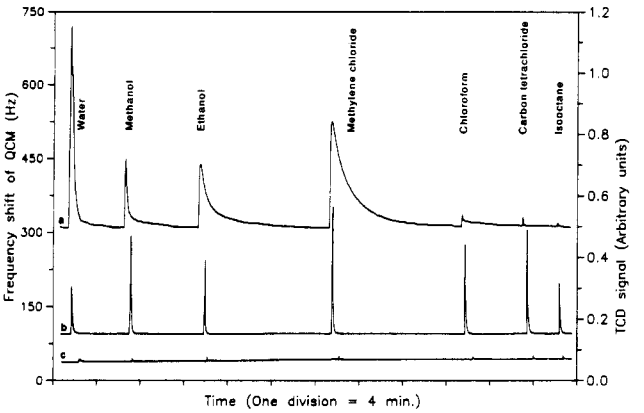

Figure 9. Transient sorption of vapor pulses on QCM coated with 29.6 $\mu g/cm^2$ silicalite, at 100 °C: (a) frequency shift of QCM/zeolite film, (b) TCD signal, (c) frequency shift of uncoated QCM.

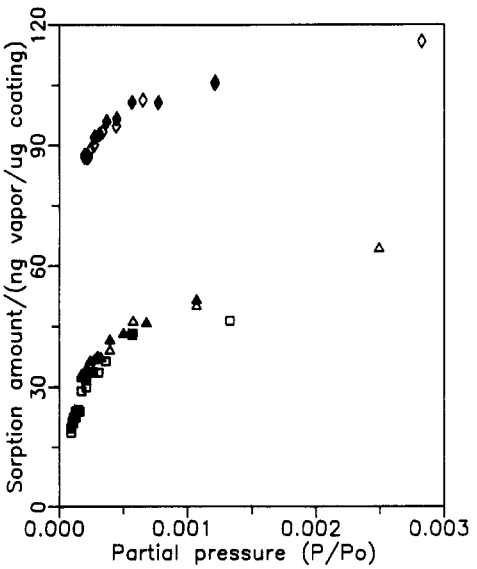

Figure 10. Sorption isotherms of water (△), *n*-hexane (□), and isooctane (◇) on a QCM coated with zeolite NaY (16.1 $\mu g/cm^2$) at 85 °C.

rejected from the coatings is in excess of 100:1. Similarly, there is a drastic difference between adsorption of CH_2Cl_2 (ca. 0.45 nm) and rejection of CCl_4 (0.59 nm). It is also observed that, in the case of molecules with kinetic diameters smaller than the zeolite pore size, the vapors are desorbed more slowly from the zeolite films compared with the TCD response. The desorption tails result from the activated diffusion/desorption processes of the probe molecules from the microporous systems. Molecules with sizes close to those of the zeolite pores desorb more slowly than smaller ones. For example, the times required for methanol and ethanol to desorb to 50% of the maximum vapor loadings are 18 and 39 s, respectively.

Zeolite NaY. With a pore size of 0.75 nm, NaY is expected to adsorb all three probe molecules at significant levels. Water, *n*-hexane, and isooctane uptakes are 0.050 (P/P_0 = 0.0011), 0.046 (P/P_0 = 0.0013), and 0.106 g/g (P/P_0 = 0.0012), respectively (Figure 10). The bulk values for saturation, measured at room temperature, are 0.35, 0.19, and 0.20 g/g for water, *n*-hexane, and isooctane, respectively.[31] The relatively high uptake of isooctane in NaY at very low pressures is probably related to its close fit to the diameter of the zeolite pores.

Transient pulse adsorptions on zeolite NaY are shown in Figure 11. Consistent with the equilibrium data, the larger isooctane molecule is now also adsorbed in the film. In comparison with the films derived from small-pore zeolites that reject isooctane (silicalite and A), this observation demonstrates the molecular sieving capabilities of the zeolite-derived films. For the molecules examined in this study, zeolite Y does not exhibit strong discrimination. However, the desorption kinetics can still differ

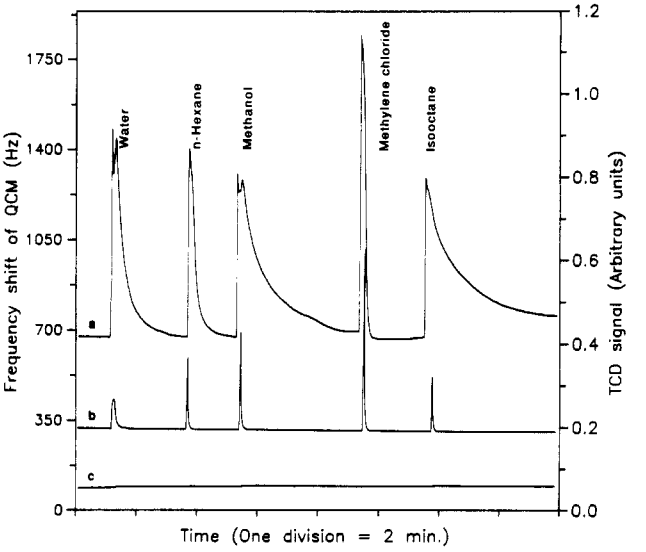

Figure 11. Transient sorption of vapor pulses on QCM coated with 33.5 $\mu g/cm^2$ zeolite NaY, at 100 °C: (a) frequency shift of QCM/zeolite film, (b) TCD signal, (c) frequency shift of uncoated QCM.

significantly, depending on size and polarity of the adsorbate. For instance, *n*-hexane (0.43 nm, 13 s is required to desorb to 50% of the maximum vapor loading) desorbs much faster than isooctane (0.62 nm, 36 s). Isooctane diffuses more slowly because its kinetic diameter is close to that of the host pores. Furthermore, desorption kinetics of polar molecules such as methanol in zeolite Y are slower than in silicalite even though the channel sizes are larger in zeolite Y. This effect is based on the stronger sorption of methanol in the polar environment of zeolite Y.

As shown above, the uptake into the films and the adsorption–desorption kinetics depend on the nature of the sorbate and its interactions with the zeolite crystals. On sorption into a specific microporous film under identical experimental conditions, the resulting peak shapes reflect physical properties of the probe molecules, such as molecular shape, size, and polarizability. Therefore, these response patterns could offer additional means of molecular identification.

Molecular Selectivity Comparing Different Zeolite Films. The different responses of the various zeolite films to the same probe molecules are an attractive basis for sensor arrays with pattern recognition capabilities. For instance, the uptake of isooctane in the Y zeolite film at P/P_0 = 0.0006 is about 100 times higher than in the silicalite film and 50 times higher than in the 3A film (0.10, 0.001, and 0.002 g/g, respectively). The uptake of *n*-hexane in the Y zeolite film at P/P_0 = 0.0013 is 19 times higher than in the 3A film (0.046 vs 0.0024 g/g), and at P/P_0 = 0.0002 it is almost 70 times higher than in the 3A film. The ratio of *n*-hexane sorption on silicalite vs 3A zeolite (0.040 vs 0.002 g/g at P/P_0 = 0.0013) becomes larger at lower vapor concentration, in agreement with the preferential filling of micropores vs external surface adsorption.[32,33] These results suggest that higher molecular size-based selectivity and larger sorption uptake (sensitivity) compared to amorphous mesoporous surfaces can be achieved at the lowest vapor concentrations, a feature of obvious importance for sensor applications.

Conclusion

In this study some unique aspects of zeolite-coated surface acoustic wave devices have been demonstrated. The coated QCMs can be used to monitor microporous adsorption behavior at very low vapor concentrations in a dynamic flow system. The high vapor sorption capacity of the microporous coatings and the molecular size- and shape-based selectivity at very low concentrations show that such a combination has potential for designing highly sensitive and selective chemical sensors.

Acknowledgment. The authors thank the National Science Foundation (Division of Materials Research) and the Department

of Energy (New Mexico WERC Program) for funding of this research. We appreciate the assistance of Kelly Brown and Ray Forrister (University of New Mexico) during various phases of this study.

Registry No. Au, 7440-57-5; N_2, 7727-37-9; H_2O, 7732-18-5; HS-$(CH_2)_3Si(OCH_3)_3$, 4420-74-0; *n*-hexane, 110-54-3; isooctane, 540-84-1.

References and Notes

(1) (a) Bein, T.; Brown, K.; Frye, G. C.; Brinker, C. J. *J. Am. Chem. Soc.* **1989**, *111*, 7640. (b) Bein, T.; Brown, K.; Frye, G. C.; Brinker, C. J. U.S. Patent Application 07/580,373; allowed on Jan 23, 1992, to be issued.
(2) Ward, M. D.; Buttry, D. A. *Science* **1990**, *249*, 1000.
(3) For recent reviews, see: (a) Janata, J. *Anal. Chem.* **1990**, *62*, 33r. (b) Hughes, R. C.; Ricco, A. J.; Butler, M. A.; Martin, S. J. *Science* **1991**, *254*, 75.
(4) Bein, T.; Brown, K.; Enzel, P.; Brinker, C. J. *Mater. Res. Soc. Symp. Proc.* **1988**, *121*, 761.
(5) Bein, T.; Brown, K.; Brinker, C. J. In *Studies in Surface Science Catalysis*; Jacobs, P. A., Van Santen, R. A., Eds.; Elsevier: Amsterdam, 1989; Vol. 49, p 887.
(6) Yan, Y.; Bein, T. *Chem. Mater.* **1992**, *4*, 975.
(7) Somorjai, G. A. *Chemistry in Two Dimensions-Surfaces*; Cornell University Press: Ithaca, NY, 1982.
(8) Bain, C. D.; Troughton, E. B.; Tao, Y. T.; Evall, J.; Whitesides, G. M.; Nuzzo, R. G. *J. Am. Chem. Soc.* **1989**, *111*, 321.
(9) Wasserman, S. R.; Biebuyck, H.; Whitesides, G. M. *J. Mater. Res.* **1989**, *4* (4), 886.
(10) Porter, M. D.; Bright, T. B.; Allara, D. L.; Chidsey, C. E. D. *J. Am. Chem. Soc.* **1987**, *109*, 3559.
(11) Li, Z.; Lai, C.; Mallouk, T. E. *Inorg. Chem.* **1989**, *28*, 178.
(12) For the 5-MHz QCM used in this experiment, a frequency shift of 1 Hz corresponds to a mass change of 17.4 ng/cm^2 on one face or 8.7 ng/cm^2 when two faces are used as in this study.
(13) King, W. H. *Anal. Chem.* **1964**, *36* (9), 1735.
(14) Hlavay, J.; Guilbault, G. G. *Anal. Chem.* **1977**, *49* (3), 1892.
(15) Ballantine, D. S.; Wohltjen, H. *Anal. Chem.* **1989**, *612* (11), 704A.
(16) This calculation is based on a nitrogen adsorption capacity of 0.239 g/g for CaA and a dense monolayer packing of nitrogen (0.162 nm^2) on the external surface at liquid nitrogen temperature.
(17) Troughton, E. B.; Bain, C. B.; Whitesides, G. M.; Nuzzo, R. G.; Allara, D. L.; Porter, M. D. *Langmuir* **1988**, *4*, 365.
(18) Allara, D. L.; Swalen, J. D. *J. Phys. Chem.* **1982**, *86*, 2700.
(19) Benziger, B.; Preston, R. E.; Schoofs, G. R. *Appl. Opt.* **1987**, *26* (2), 343.
(20) Brunauer, S.; Emmett, P. H.; Teller, E. *J. Am. Chem. Soc.* **1938**, *60*, 309.
(21) Gregg, S. J.; Sing, K. S. W. *Adsorption, Surface Area and Porosity*, 2nd ed.; Academic: New York, 1982.
(22) Ricco, A. J.; Frye, G. C.; Martin, S. J. *Langmuir* **1989**, *5*, 273.
(23) Ishida, H.; Koenig, J. L. *J. Colloid Interface Sci.* **1978**, *64* (3), 555.
(24) Chiang, C. H.; Ishida, H.; Koenig, J. L. *J. Colloid Interface Sci.* **1980**, *74* (2), 396.
(25) Schrader, M. E. *J. Colloid Interface Sci.* **1984**, *100*, 512.
(26) Janczuk, B.; Bialopiotrowicz, T.; Chibowski, E.; Dawidowicz, A.; Kliszcz, A. *J. Mater. Sci.* **1990**, *25*, 1682.
(27) Szostak, R. *Molecular Sieves, Principles of Synthesis and Identification*; Van Nostrand Reinhold: New York, 1988.
(28) Barrer, R. M. *Hydrothermal Chemistry of Zeolites*; Academic: New York, 1982.
(29) Gregg, S. J.; Sing, K. S. W. *Adsorption, Surface Area and Porosity*, 2nd ed.; Academic Press: New York, 1982; Chapters 2 and 4.
(30) Carrott, P. J. M.; Sing, K. S. W. *Chem. Ind.* **1986** (Nov 17), 786.
(31) Breck, D. W. *Zeolite Molecular Sieves*; Wiley: New York, 1974.
(32) Carrott, P. J. M.; Roberts, R. A.; Sing, K. S. W. In *Characterization of Porous Solids*; Unger, K. K., Rouquerol, J., Sing, K. S. W., Kral, H., Eds.; Elsevier: Amsterdam, 1988; p 88.
(33) Kakei, K.; Ozeki, S.; Suzuki, T.; Kaneko, K. *J. Chem. Soc., Faraday Trans. 1* **1990**, *80* (2), 371.

Structure and Catalytic Activity of Alumina Supported Platinum–Cobalt Bimetallic Catalysts. 3. Effect of Treatment on the Interface Layer

Zoltán Zsoldos and László Guczi*

Surface Science and Catalysis Laboratory, Institute of Isotopes of the Hungarian Academy of Sciences, P.O. Box 77, H-1525 Budapest, Hungary *(Received: February 25, 1992)*

The structure of the interface between metal and alumina in a series of $Pt_{1-x}Co_x/Al_2O_3$ bimetallic samples has been investigated by X-ray photoelectron spectroscopy (XPS) after calcination in oxygen at 770 K with subsequent in situ reduction in hydrogen at 770 K. On all calcined samples platinum was found in the Pt(4+) valence state as an oxide species. Subsequent treatment in H_2 at 770 K resulted only in a partial reduction of ionic platinum into the zerovalent state. The remaining platinum found in the Pt(2+) form is strong evidence of metal–support interaction affecting the platinum–alumina system. After calcination Co_3O_4 and the cobalt surface phase (CSP), depending upon the cobalt content of the samples, were found to be the predominant species. Starting from a pure cobalt sample ($x_{Co} = 1.0$), the initial decrease in dispersion of the oxidized cobalt phases is interpreted by the effect of platinum (or chlorine). On these bimetallic samples, the dispersion of the Co_3O_4 phase forming three-dimensional particles was decreased, which also contributes to the enhanced cobalt reducibility. After reduction on the samples with low cobalt content, formation of $CoPt_3$ bimetallic particles was clearly demonstrated. Along with this result, a prediction of the possible catalytic behavior of $Pt_{1-x}Co_x/Al_2O_3$ catalysts of various surface compositions is discussed. The results are compared with those obtained earlier in the case of treatments at 570 K (*J. Phys. Chem.* **1991**, *95*, 798).

Introduction

Modification of supported cobalt catalyst has been a subject of several investigations. These studies are primarily concerned with the increased selectivity toward oxygenates in CO hydrogenation. Alkaline earth metals,[1] Ru and Re,[2] as well as other transition metals,[3] were found to promote silica supported cobalt catalysts for increased yield of C_{2+}-alcohol. Supported cobalt, in which metallic Co^0 and the support were interfaced by a cobalt(2+) oxide layer, was also observed to facilitate alcohol formation.[4] In addition to the effect of the support, even the various form of cobalt precursors (nitrate, chloride, acetate, and carbonyl cluster)[1,5,6] influenced this interface by modifying the reducibility of cobalt, thereby controlling the Co^0/CoO ratio.

These studies indicated that selectivity is a very sensitive function of the Co/support interface. In addition to the effect of various additives, a dedicated balance among the various cobalt species depends also upon the reduction conditions. At low temperature reduction, only a small fraction of cobalt ions is transformed into zerovalent cobalt, whereas at a too high temperature the CoO/Al_2O_3 and Co_3O_4/Al_2O_3 systems can be converted into an almost irreducible $CoAl_2O_4$ spinel phase.[7] On the other hand, addition of noble metals of group VIII transition metals (Pt,[8-11] Pd,[12] or Ir[13]) may help the reduction of cobalt; however, formation of the bimetallic particles has not unambiguously been proven.

In earlier studies it was found that in the $Pt_{1-x}Co_x/Al_2O_3$ samples[14,15] after calcination at 570 K followed by reduction at

0022-3654/92/2096-9393$03.00/0